This article has been accepted for publication in a future issue of this journal, but has not been fully edited. Content may change prior to final publication. Citation information: DOI 10.1109/TIE.2018.2868304, IEEE Transactions on Industrial Electronics

Improved Harmonic Performance of Cascaded H-Bridge Converters with Thermal Control

Vito Giuseppe Monopoli, *Senior Member*, *IEEE*, Abraham Marquez, *Member*, *IEEE*, Jose I. Leon, *Felow Member*, *IEEE*, Youngjong Ko, *Student Member*, *IEEE*, Giampaolo Buticchi, *Senior Member*, *IEEE* and Marco Liserre, *Fellow Member*, *IEEE*.

***Abstract*—Among multilevel converter topologies, the cascaded H-bridge converter (CHB) is one suitable solution for multiple applications such as flexible ac transmission systems and motor drives. CHB presents a natural high modularity because it is formed by the serial connection of H-bridges. This paper deals with a CHB where the cells do not have the same aging because the maintenance during the years of operation forces to replace some damaged cells of the converter with new or repaired ones. A method based on clamping one power cell can be used to reduce the power losses of that cell reducing its temperature and increasing its lifetime. However, clamping one cell of the CHB introduces high harmonic distortion around twice the carrier frequency due to the CHB unbalanced operation when a conventional phase-shifted PWM is applied. A deep harmonic distortion analysis of the CHB output voltage with thermal control based on clamping one cell is presented. Using this analysis, the harmonic distortion at twice the carrier frequency is eliminated applying a non-conventional phase-shifted PWM where the angles between the carriers of consecutive power cells are modified. Experimental results show how the thermal control applying the clamping of a power cell is achieved whilst the harmonic distortion around twice the carrier frequency is eliminated.**

***Index Terms*—Harmonic analysis, Pulse width modulation, Multilevel converters.**

I. Introduction

The use of multilevel converters has become a reality in the last decades for a wide variety of power applications such as fans, pumps, variable frequency drives, power quality applications and renewable energy integration, among others [1], [2]. One of the most well-known converter topologies is the cascaded H-bridge converter (CHB), which was proposed by McMurray in 1971 [3]. CHB is composed by the serial connection of H-bridges as shown in Fig. 1 where a three-cell CHB is represented. The basic power cell is usually the H-bridge, however in the literature other power cells like NPC or T-type can be found [4]. In this way, this topology is able to achieve very high nominal voltages with a large number of output voltage levels with high modularity and natural fault-tolerant capability. These good features make the CHB one of the most used topologies for medium and high-voltage applications with an excellent quality in the output voltage and current [5]. In fact, CHB is very popular in countries where medium voltage grids above 6.6 kV.

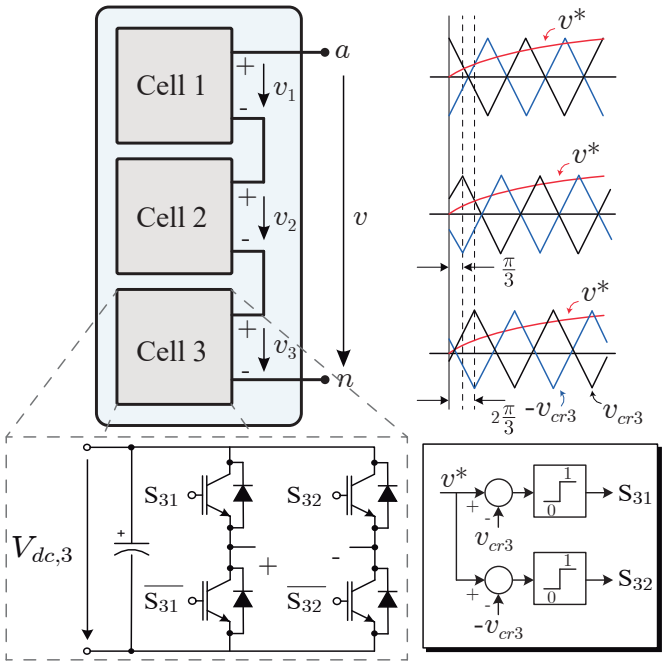

Fig. 1: Three-cell multilevel cascaded H-bridge converter (CHB): Topology and conventional PS-PWM modulation technique

A. CHB Converter Description and Operation

The conventional way to operate the CHB is to apply the conventional phase-shifted pulse-width modulation (PS-PWM) method. Each power cell is usually operated by a

Manuscript received Feb 20, 2018; revised April 24, 2018 and July 04, 2018; accepted August 12, 2018.

The authors gratefully acknowledge financial support provided by the Spanish Science and Innovation Ministry under project TEC2016-78430-R. Section II was made possible by NPRP 9-310-2-134 from the Qatar National Research Fund (a member of Qatar Foundation). The statements made herein are solely the responsibility of the authors.

V. G. Monopoli is with the Department of Electrical and Information Engineering, Politecnico di Bari, 70126 Bari, Italy (e-mail: vitogiuseppe.monopoli@poliba.it).

A. Marquez and Jose I. Leon are with the Electronic Engineering Department, Universidad de Sevilla, Seville, 41092 Spain (e-mail: amarquez@ieee.org).

Y. Ko and M. Liserre are with the Chair of Power Electronics, Christian-Albrechts-University of Kiel, Kiel 24143, Germany (e-mail: yoko@tf.uni-kiel.de; ma@tf.uni-kiel.de; ml@tf.uni-kiel.de).

G. Buticchi is with the University of Nottingham Ningbo China, Ningbo 315100, China (e-mail: giampaolo.buticchi@nottingham.edu.cn).

conventional unipolar PWM with carrier frequency equal to f_c and triangular carriers between consecutive power cells have a phase shift displacement. This phase displacement between consecutive triangular carriers is conventionally defined as π divided by the number of H-bridges of the CHB phase, denoted by N [6]. To support this basic idea, unipolar PWM and PS-PWM concepts are also introduced in Fig. 1 for the three-cell CHB topology.

PS-PWM applied to CHB presents multiple advantages. It achieves a natural multiplicative effect of the switching frequency of the output voltage. If the triangular carriers of each unipolar PWM have a frequency equal to f_c, the effective switching frequency of the output voltage is $2Nf_c$. In addition, PS-PWM naturally achieves a power equalization [7] of the power cells of the CHB because the voltage reference of all H-bridges is the same. This fact leads to a natural equalization of power devices temperature which comes with equally distributed aging. The conventional operation of a CHB using the PS-PWM technique can be observed in Fig. 2 from 0 to $40ms$ where the voltages of the three cells are 150 V and the modulation indices are 0.8.

B. CHB Maintenance and its Effect on the Aging

Thermal stress is the main cause of aging, and hence, the principal cause of failure due of fatigue generated in the solder joints inside devices. Repetition of thermal cycles provoke the expansion and compression of materials leading to the increase of thermal resistance and it generate more thermal stress [8]–[10]. Remaining device lifetime is a very important parameter because the maintenance and operation cost are directly dependent of it. In this way, many authors and manufacturers are focusing on the study of predictive models to obtain the remaining lifetime as function of cumulative thermal cycles [11], [12].

Fault-tolerant capability is a very important factor for industry because it lets to continue operating the power converter even if a fault occurs. CHB presents a high-modularity and natural fault-tolerant capability. It means that the maintenance operations are straight-forward because if a power device fails, its H-bridge can be bypassed permitting the power converter operation [13]. The broken power cell can be easily replaced by a new one, sending it to be repaired if possible. This operation is very positive from the maintenance point of view, keeping the CHB converter always on operation.

However, after a maintenance operation replacing a power cell in the CHB, a problem related to the different aging of the power cells is introduced. The power cell that replaces the broken one has a different aging compared with all the other power cells. With years of operation, a non-negligible different aging between all the power cells of the CHB appears [14].

II. CHB Active Thermal Control

Active Thermal Control (ATC) is a technique that allows modifying the thermal stress of the power modules by changing the electrical parameters of the converter [10]. At it is shown, power cycling is one of the main causes of failure for power modules and industry and academia have been studying the phenomenon in depth. Lifetime models that predict the number of sustainable power cycles at specific average temperatures with a certain amplitude are available in the technical literature [15].

Modifying the control parameters, as an example switching frequency, capacitor voltages and modulation indexes, [10] can change the power loss, decreasing the thermal cycle amplitude and the effects in terms of lifetime extension can be predicted with the available lifetime models. In the following, two possibilities are deeply analyzed. At it will be shown, when the CHB cells are operated with different control parameters, an increase of the THD voltage is noticeable.

One possible option to mitigate the non-equalized aging effect is to apply a different modulation index to each power cell. So, more damaged cells would generate less voltage than the new ones. As the same current flows through all power cells, each power cell delivers a different level of power leading to improve the average aging of the power cells. The more damaged cells will operate with reduced modulation index and the less damaged cells compensate it increasing their modulation index values [16]. This can be observed in Fig. 2a from 40 to $80ms$.

A second option is to deal with the switching losses of each power cell. In this way, it is possible to clamp the more damaged cells generating the maximum voltage during a portion of the fundamental period [17]. Remaining cells have to compensate it decreasing their reference voltages. This second option has been also represented in Fig. 2a from 80 to $120ms$. As a drawback, during the clamping time the CHB converter operates with less voltage levels increasing the current ripple.

These two methods can be applied in order to achieve an active thermal control, which means that those methods can manage the temperature of the converter power devices. It can be noticed that both methods applied to the CHB are complementary and can be applied simultaneously if required.

The effectiveness of the Active Thermal Control in affecting the lifetime of the power electronics, effectively reducing the spread of the end-of-life has been demonstrated in previous publications [18], [19]. Monte Carlo simulations can also be an effective tool to analyze the sensitivity of the converter lifetime to parameter variation [20].

One drawback of both active thermal control methods (modification of the modulation indexes or clamping) is that the CHB operates under unbalanced conditions and the conventional PS-PWM does not work so efficiently as expected. This phenomenon can be observed taking into account the harmonic spectrum of the output voltage represented in Fig. 3. If the clamping method active thermal control is active, a non-negligible harmonic distortion appears at $2f_c$.

This fact has been studied by researches in past years and some modulation techniques have been proposed. A part of them are based on the feed-forward idea considering real dc voltages to carry out some calculations in order to determine the duty cycles. As example, this technique is the base of methods presented in [21], [22] for PS-PWM and [23]–[27] for the well-known space-vector modulation technique. However,

This article has been accepted for publication in a future issue of this journal, but has not been fully edited. Content may change prior to final publication. Citation information: DOI 10.1109/TIE.2018.2868304, IEEE Transactions on Industrial Electronics

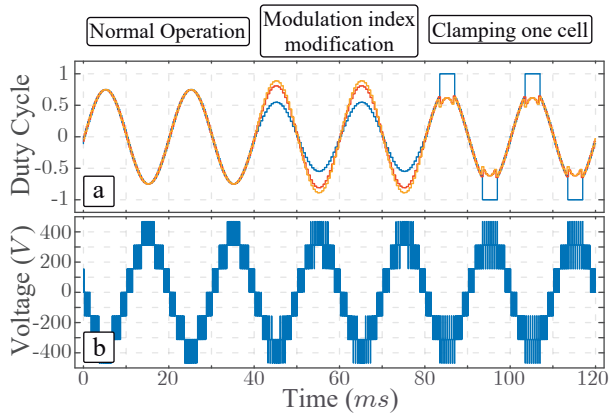

Fig. 2: Operation of the three-cell CHB under several conditions: 0-40 ms balanced operation, 40-80 ms unbalanced operation with different modulation indices, 80-120 ms unbalanced operation based on cell clamping. From top to bottom a) Duty Cycle applied in each cell. b) CHB output voltage.

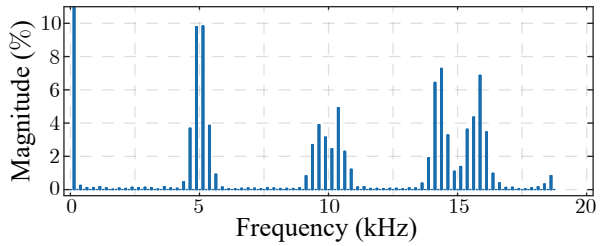

Fig. 3: Spectrum magnitude of the CHB output voltage under PS-PWM operation with one clamped cell.

these proposel does not deal with the distortion generated at $2f_c$.

Whenever such balanced conditions are not met, the conventional PS-PWM fails and different solutions have been proposed in literature to fit the carrier phase shifting to this kind of operation. For instance, the technique proposed in [28] can be considered an extension of the classical PS-PWM to the case of unequal dc voltages and it achieves the best possible harmonic cancellation through an asymmetrical carrier phase-shifting. The same asymmetrical PS-PWM proposed in [28] is investigated with more details in [29]. In fact, harmonic cancellation capability of such technique is assessed as well as the upper limit for the equivalent switching frequency. Another adaptation of the classical PS-PWM is presented in [30]. In particular, the proposed asymmetrical carrier phase shifting addresses the case of equal dc voltages which tend to become unbalanced because of different power levels managed by the H-bridges or different power losses. Unlike [28], this technique allows the best harmonic cancellation in case of different modulating signals that have to be used to implement the dc-link voltage balance control. The Fourier series of the pulses, produced in each PWM period by the H-bridges, is used in [31] to carry out the variable carrier phase shifting. In this case the cancellation of the fundamental harmonic of the pulses produced in every carrier period by each H-bridge is achieved. This technique can cope with unequal modulating signals and unequal dc voltages.

In this paper, as the main contribution, an improvement of the active thermal control based on clamping one H-bridge of the CHB will be presented. The aim of the proposed method is to eliminate the undesirable harmonic distortion present at $2f_c$ modifying the conventional PS-PWM method in order to achieve ATC without deteriorating the power quality. The way to achieve this goal is based on determining every fundamental period the corresponding phase displacements between carriers of adjacent H-bridges.

III. Harmonic Analysis of the Converter Output using PS-PWM with One Clamped Cell

A. Clamped Cell Output Voltage Description

Assuming the normalized reference voltage for the clamped cell shown in Fig. 4a, it is possible to undergo a harmonic analysis of its output voltage and to derive, after considerable mathematical manipulations, its analytical expression with all the harmonic components, where the factor $Z(x)$ is introduced in order to simplify the expressions:

$$Z(x) = \frac{\sin(x\phi)}{x} \tag{1}$$

.

From expression (8), it is possible to notice that the carrier harmonics are never present and the sideband harmonics do not exist in the odd carrier groups. Therefore, odd carrier groups are completely eliminated and hence only even carrier groups still exist. In these groups only odd sideband harmonics exist. Using the expression (8) it is possible to plot the trend of the normalized fundamental harmonic as a function of the clamping angle ϕ for different values of the modulation index M_c as shown in Fig. 4c. It is evident that also with this technique it possible to extend the loading capability over 1 and even further 1.15.

B. Non-clamped Cell Output Voltage Description

Assuming a three-cell CHB with one clamped cell and two non-clamped cells, the normalized reference voltage to be used for the non-clamped cells is shown in Fig. 4b. Also in this case a harmonic analysis of the switching cell output voltage has been carried out and results are summarized in the analytical expression (9).

Using the expression (9) it is possible to plot the trend of the normalized fundamental harmonic as a function of the clamping angle ϕ for different values of the modulation indices M_i and M_c as shown in Fig. 5. It is clear that the first harmonic of the non-clamped cells depend both on the clamping angle ϕ and on the modulation index of the clamped cell M_c. The loading capability of the switching cells decreases as the clamping angle grows up and the modulation index of the non-switching cell decreases. Moreover, it is possible to notice that only modulation index values $M_i > 0.5$ guarantee always a positive value of the first harmonic amplitude. For the lower values of the modulation index it exists a particular value of the clamping angle beyond which negative values

This article has been accepted for publication in a future issue of this journal, but has not been fully edited. Content may change prior to final publication. Citation information: DOI 10.1109/TIE.2018.2868304, IEEE Transactions on Industrial Electronics

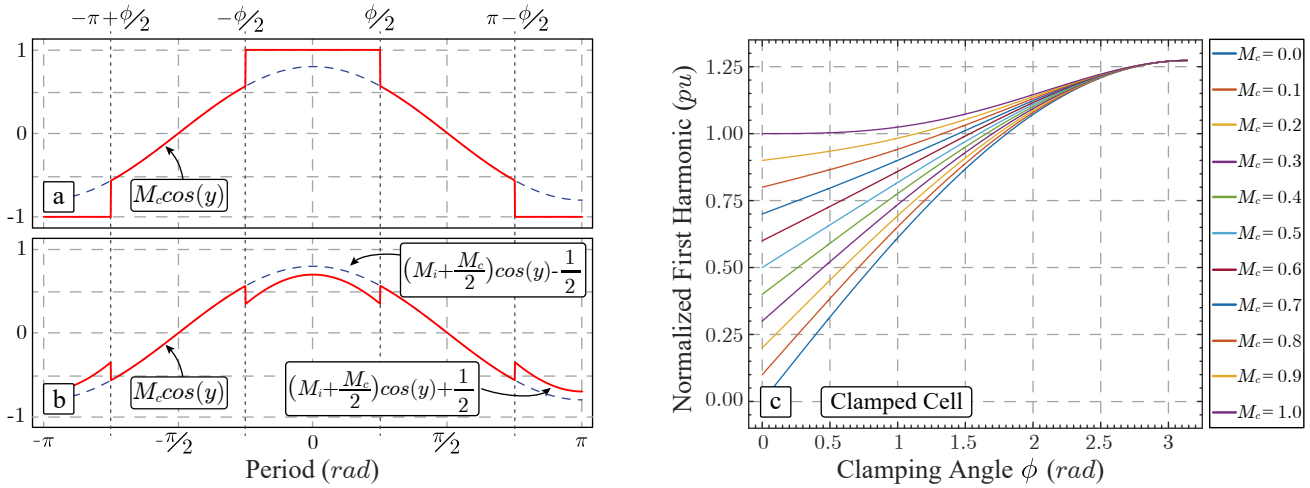

Fig. 4: Normalized reference voltage of a) the clamped cell b) the non-clamped cells. (c) Normalized first harmonic depending on the clamping angle ϕ of a clamped cell.

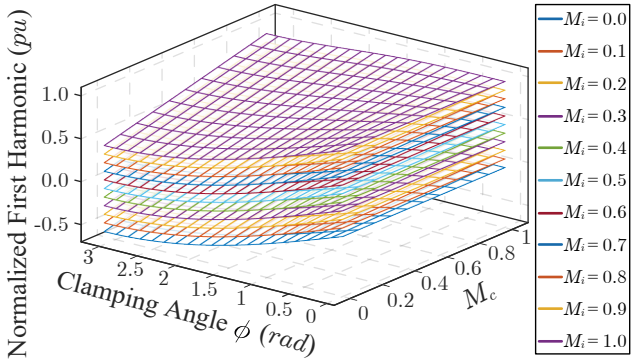

Fig. 5: Normalized first harmonic content of the output voltage of a non-clamped cell depending on the clamping angle (ϕ) and modulation index of the clamped cell (M_c) and the non-clamped cell (M_i).

of the first harmonic occur (i.e. phase opposition). Therefore, beyond this limit the cell changes its power processing attitude (i.e. a power flow direction change occurs).

C. Total CHB Output Voltage Description

Assuming two non-clamped cells and just one clamped cell, the harmonic components of the CHB output voltage can be expressed by expression (10), where M_c is the modulation index of the clamped cell, M_i is the modulation index of the i^{th} non-clamped cell, V_c^{dc} is the dc voltage of the clamped cell, V_i^{dc} is the dc voltage of the i^{th} non-clamped cell, ω_0 is the pulsation of the modulating signal, m and n are indices to account for baseband, carrier and sideband harmonics, J_{2n-1} is the Bessel function of order $2n-1$, ω_c is the pulsation of the carrier signal and θ_i is the carrier phase of the i^{th} non-clamped cell with respect to the carrier phase of the clamped cell.

IV. Harmonic Analysis Results

Taking into account the previous harmonic analysis, the normalized spectrum of the total output voltage generated by the CHB has been obtained considering the conditions reported in Table I.

An equally spaced carrier phase (equal to the conventional value defined by the PS-PWM method) with phase displacements equal to $\theta_1 = \pi/3$ and $\theta_2 = 2\pi/3$ have been considered. Figure 6a shows the normalized harmonic spectrum of the CHB output voltage with the clamping angle $\phi = 60°$. In this unbalanced case, it is not achieved any harmonic cancellation.

V. Variable-angle PS-PWM for three-cell CHB with one clamped cell

It could be possible to implement a suitable phase shift of the carriers in order to achieve the cancellation of the sideband harmonics that more deeply influence the WTHD0 value ("Main Harmonics"). In fact, in this case, the cancellation condition is not the same for all the harmonics belonging to the same carrier group and hence a whole carrier group can not be cancelled all at once. The sidebands to be cancelled are the ones right next the missing carrier of the first carrier group ($m = 1$ and $n = 0$), leading to determine expressions (2) and (3) from (8) and (9) respectively.

The cancellation of the Main Harmonics occurs if the following conditions are met.

TABLE I: Parameter Values under Unequal dc Voltages and Unequal Modulating Signals

Parameter	Value
Number of cells in the CHB	3
Cell switching frequency f_c (kHz)	1
DC voltages $[V_c^{dc}, V_1^{dc}, V_2^{dc}]$ (V)	$[810, 720, 840]$
Modulation indices $[M_c, M_1, M_2]$	$[0.55, 0.9, 0.95]$

This article has been accepted for publication in a future issue of this journal, but has not been fully edited. Content may change prior to final publication. Citation information: DOI 10.1109/TIE.2018.2868304, IEEE Transactions on Industrial Electronics

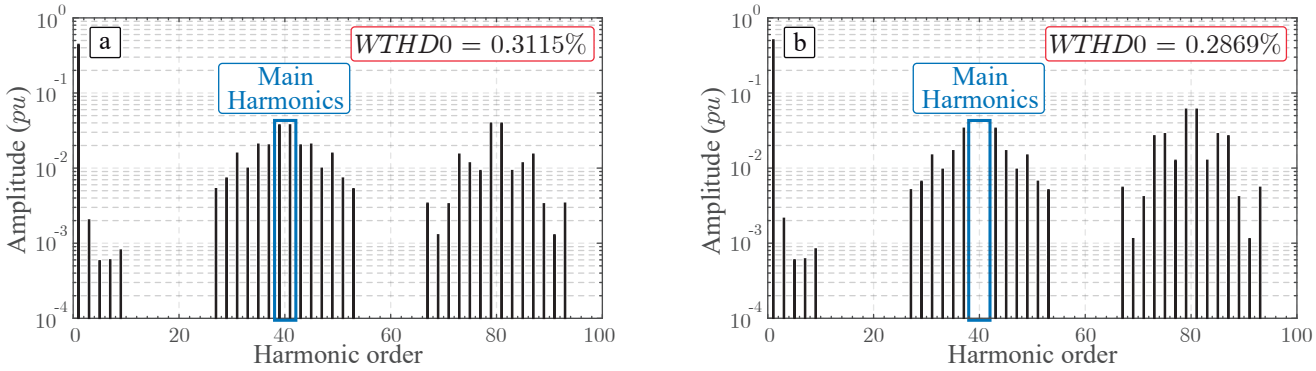

Fig. 6: Spectrum analysis for multilevel CHB with a clamped power cell with $\phi = 60°$ applying a) conventional PS-PWM b) proposed variable-angle PS-PWM.

$$V_c = \frac{2V_c^{dc}}{\pi^2}\left[J_{-1}(\pi M_c)\Big(\pi - \phi - Z(1)\Big) - \sum_{k=2}^{\infty} J_{2k-1}(\pi M_c)cos(k\pi)\Big(Z(k-1) + Z(k)\Big)\right] \tag{2}$$

$$\begin{aligned} V_i = \frac{2V_i^{dc}}{\pi^2}\Bigg[& J_0\Big(\pi\Big(M_i + \frac{M_c}{2}\Big)\Big)Z(1/2) + J_1(\pi M_i)\Big(Z(1) - \pi + \phi\Big) \\ & + \sum_{k=2}^{\infty} J_k\Big(\pi\Big(M_i + \frac{M_c}{2}\Big)\Big)\Big[cos\Big((k-1)\pi\Big)sin\Big((k+3)\frac{\pi}{2}\Big) + sin\Big((k+1)\frac{\pi}{2}\Big)\Big]\Big[\frac{1}{2}Z\Big(\frac{k-1}{2}\Big) + \frac{1}{2}Z\Big(\frac{k+1}{2}\Big)\Big] \\ & - \sum_{k=2}^{\infty} J_k\Big(\pi M_i\Big)\Big[sin\Big((k+2)\frac{\pi}{2}\Big)\Big(1 + cos[(k-1)\pi]\Big)\Big[\frac{1}{2}Z\Big(\frac{k-1}{2}\Big) + \frac{1}{2}Z\Big(\frac{k+1}{2}\Big)\Big]\Big] \end{aligned} \tag{3}$$

$$\begin{aligned} V_c + V_1 cos(\varphi_1) + V_2 cos(\varphi_2) = 0 \\ V_1 sin(\varphi_1) + V_2 sin(\varphi_2) = 0 \end{aligned} \tag{4}$$

where $\varphi_1 = 2\theta_1$ and $\varphi_2 = 2\theta_2$ are respectively the displacement angles between the main harmonics of the first/second non-clamped cell and the main harmonic of the clamped cell. The solution to expression (4) is:

$$\begin{aligned} cos(\varphi_1) = \frac{1}{2}\frac{-V_c^2 - V_1^2 + V_2^2}{V_c V_1} \\ cos(\varphi_2) = \frac{1}{2}\frac{-V_c^2 + V_1^2 - V_2^2}{V_c V_2} \end{aligned} \tag{5}$$

Valid solutions for the displacement angles φ_1 and φ_2 are obtained only if the following conditions are met:

$$\begin{aligned} |V_c - V_1| \leq V_2 \leq (V_c + V_1) \\ |V_c - V_2| \leq V_1 \leq (V_c + V_2) \end{aligned} \tag{6}$$

This analysis has been taken into account in order to eliminate the "main harmonics" (harmonic distortion located at $2f_c$) applying a variable-angle PS-PWM with phase displacement angles determined by expression (5). It is very important to notice that the calculation of the phase displacement angles using expressions (2), (3) and (5) has to done every fundamental period (usually 20 miliseconds). In addition, to obtain the angles (φ_1,φ_2) only values of $k \leq 10$ are required to be included in the calculations reducing the computational cost of (2) and (3). Factors with higher values of k are negligible and can be discarded. Taking into account these facts, although the calculations are not simple, the computational burden is acceptable and does not represent a problem of the method.

In order to test the proposed method, the obtained harmonic spectrum of the output voltage with the CHB working with parameters of Table I and ϕ equal to $60°$ is represented in Fig. 6b. The harmonic located at $2f_c$ are eliminated using the proper phase displacement angles calculated by the proposed method (φ_1=$2\theta_1$=94.02°, φ_1=$2\theta_1$=245.26°).

It is possible to notice that the proposed method allows to lower the $WTHD0$ value from 0.3115% to 0.2869% which means approximately a 8% reduction. Since the $WTHD0$ can inherently take into consideration the effect that a given voltage harmonic produces on the corresponding current harmonic, the achieved reduction shows that the proposed solution can effectively limit the low order voltage harmonics that have a major influence on the current waveform distortion. Therefore, assuming that the AC filter parameters are not changed, this reduction of the $WTHD0$ produces its beneficial effects on the current quality. On a different perspective, the achieved improvement of the $WTHD0$ allows for the AC filter size reduction keeping the same current waveform quality.

VI. Experimental Results

In order to check the good performance of the proposed active thermal control with improved harmonic distortion

This article has been accepted for publication in a future issue of this journal, but has not been fully edited. Content may change prior to final publication. Citation information: DOI 10.1109/TIE.2018.2868304, IEEE Transactions on Industrial Electronics

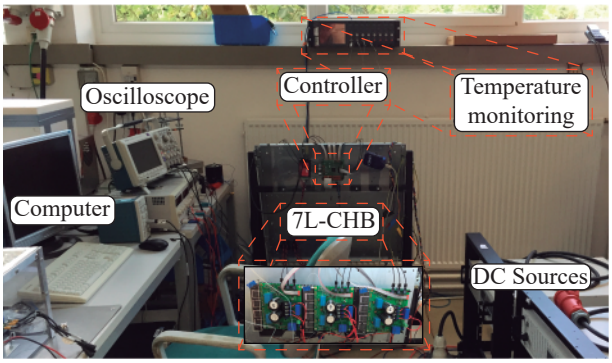

Fig. 7: Complete experimental setup composed by Three-cell CHB, temperature monitoring and DC sources.

response, some experimental results have been taken in the laboratory prototype which is shown in Fig. 7. The power devices which compose the basic power cell are IXYB82N120C3H1 from IXYS and the whole power system is managed by MPC5643L microprocessor from NXP. Moreover, the most important passive elements values and parameters that take part of this experiment are shown in Table II.

From the frequency domain point of view, the obtained results are shown in Fig. 8 where the CHB output voltage and the corresponding harmonic spectrum is represented. In the experiment, as can be consulted in Table II, the CHB converter operates with unbalanced dc voltages $\left([134, 130, 140]V\right)$ and different modulation indices $\left([0.5, 0.9, 1.0]\right)$.

At the beginning of the experiment, the CHB is operated clamping the first cell with $\phi = 60°$ and applying the conventional PS-PWM method. The resulting output voltage harmonic spectrum are represented in Fig. 8a being easy to see the distortion provoked by the unbalanced operation. After that, the variable-angle PS-PWM technique is applied under the same unbalanced conditions leading to the following displacement angles, $\varphi_1 = 109.80°$ and $\varphi_2 = 262.96°$. The corresponding harmonic spectrum using the variable method is also included in Fig. 8c. In blue, it is represented the result using the conventional PS-PWM method whereas the result using the proposed modification of the PS-PWM technique is drawn in red. It is clear that the main harmonic distortion present at $2f_c$ is completely eliminated when the proposed modification is applied. Moreover, in Fig. 8b and Fig. 8d, a detail of the low order voltage spectrum is shown where it can be clearly observed that the low order components are not affected.

TABLE II: CHB parameters setup, passive elements and unbalanced operation point considered for the experiment.

Parameter	Value
Number of cells in the CHB	3
Cell switching frequency f_c (kHz)	10
Cell DC Capacitance (mF)	2.2
DC voltages $[V_c^{dc}, V_1^{dc}, V_2^{dc}]$ (V)	$[134, 130, 140]$
Modulation indices $[M_c, M_1, M_2]$	$[0.5, 0.9, 1.0]$
Clamping angle ϕ $(°)$	60
Load Inductance (mH)	0.3
Load Resistance (Ω)	10

In order to validate the effect of the clamping angle in combination with the proposed methodology on the thermal behavior of the CHB, in Fig. 9 the device case temperature of each power cell are shown under a constant ambient temperature of $23°C$. Until $t = 48$ minutes the power converter is conventionally operated reaching each power cell approximately 37.5, 36.8 and $35.2°C$, respectively. Afterward,the proposed method with $60°$ clamping angle is applied in one H-bridge from $t = 48$ to $t = 58.5$ minutes, leading in a significant temperature reduction of $1.1°$ in the clamped cell whereas the remaining cells are unaffected. This experiment demonstrates that the proposed method enables to improve the harmonic performance facilitating the active thermal control.

VII. Conclusions

Reducing as much as possible the maintenance costs are a key factor of industrial power converters based products. Prognostic maintenance should be implemented in order to improve the power converter operability. In a modular structure such as the CHB, the possibility to delay the failure of one cell by means of active thermal control could allow implementing planned maintenance. Unfortunately, active thermal control methods introduces harmonic distortion at low frequency which is a drawback in terms of output waveforms filtering costs.

In this paper, a method to reduce this problem is presented. The method is based on a modification of the conventional PS-PWM technique where the phase displacement angles between consecutive power cells is not fixed. The calculation of the phase displacement angles to be applied is based on the Fourier analysis of the power cell waveforms. The calculations have to be carried out every fundamental period so the computational burden is limited.

The proposed method is suited to be applied to three-cell CHB converters. CHB converters are a mature comercial product for high-power applications becoming a very well-suited mainly for high-power motor drives and flexible ac transmission systems (FACTS). In fact, many CHB comercial converters can be found in the market, some of them formed by the serial connection of three H-bridges. As commercial industrial solutions, RMVC 5100 (3kV class) by RXPE and MVW3000 (3kV class) by WEG can be found as CHB converters formed by three-cells. The applicability of the proposed method is direct in these commercial products using a thermal measurement in each cell (normally already available for safety purposes).

Experimental results validate the proposed method showing that the thermal control of the CHB topology can be done and the harmonic distortion around twice the carrier frequency is eliminated. The results show how the proposed strategy improves the harmonic spectra of the output waveforms without affecting the thermal control.

Appendix

In this section the equation set resulting from the mathematical analysis of the CHB converter operating with one clamped

This article has been accepted for publication in a future issue of this journal, but has not been fully edited. Content may change prior to final publication. Citation information: DOI 10.1109/TIE.2018.2868304, IEEE Transactions on Industrial Electronics

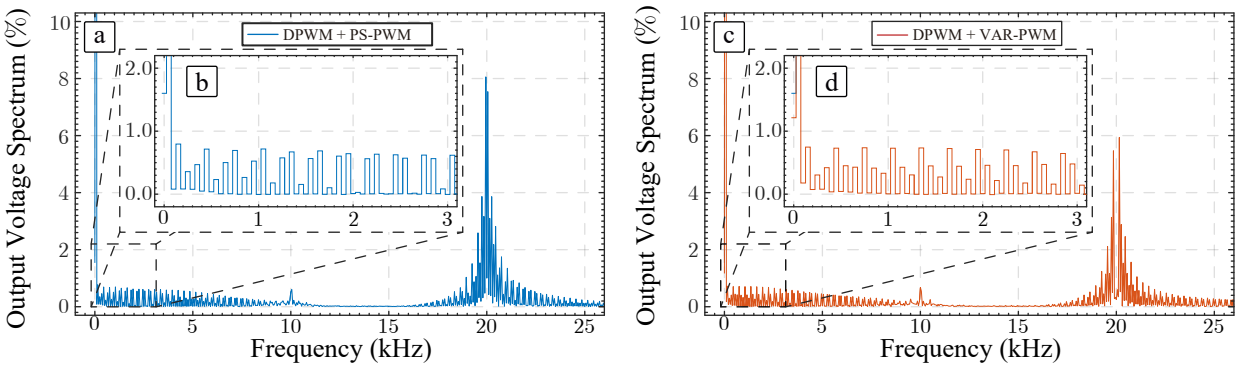

Fig. 8: Experimental results: Harmonic spectrum under the unbalanced operation point provided by Table II. a) Conventional PS-PWM technique. b) Enlarged low order detail. c) Proposed variable-angle PS-PWM. d) Enlarged low order detail.

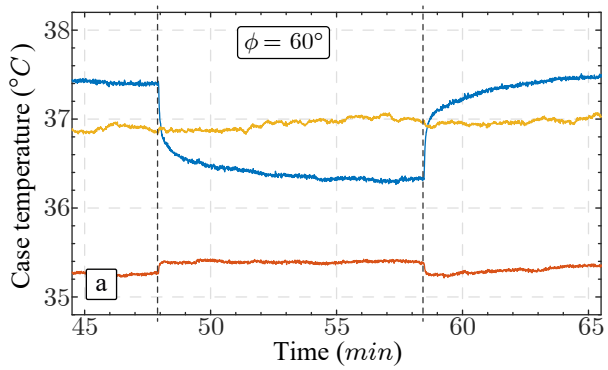

Fig. 9: Thermal experimental results. Case temperature measurement of power devices in each power cell. The color scheme is as follows: first cell in blue, second cell in red and third cell in yellow.

cell is compiled.

It has to be noticed that all the expressions have been simplified using the coefficients presented in (7). Equation (8) shows the output voltage of an H-bridge which is operated by a D-PWM modulation technique clamping it during ϕ radians as shown in Fig. 4a. On the other hand, in (9) the output voltage of a non-clamped HB cell is shown. Finally, the complete output voltage expression of the CHB under ATC operation using D-PWM modulation technique is presented in (10) determined by the sum of expressions (8) and (9).

$$\begin{aligned} a &= 2n-1 \qquad b = n-1 \qquad c = m+n-1 \\ d &= n+k-1 \qquad e = n-k \end{aligned} \tag{7}$$

REFERENCES

[1] S. Kouro, M. Malinowski, K. Gopakumar, J. Pou, L. G. Franquelo, B. Wu, J. Rodriguez, M. A. Perez, and J. I. Leon, "Recent advances and industrial applications of multilevel converters," *IEEE Transactions on Industrial Electronics*, vol. 57, no. 8, pp. 2553–2580, Aug 2010.

[2] M. Malinowski, K. Gopakumar, J. Rodriguez, and M. A. Perez, "A survey on cascaded multilevel inverters," *IEEE Transactions on Industrial Electronics*, vol. 57, no. 7, pp. 2197–2206, July 2010.

[3] W. Mcmurray, "Fast response stepped-wave switching power converter circuit," May 25 1971, uS Patent 3,581,212. [Online]. Available: https://www.google.com/patents/US3581212

[4] P. Kakosimos and H. Abu-Rub, "Predictive control of a grid-tied cascaded full-bridge npc inverter for reducing high-frequency common-mode voltage components," *IEEE Transactions on Industrial Informatics*, vol. PP, no. 99, pp. 1–1, 2017.

[5] J. Rodriguez, J.-S. Lai, and F. Z. Peng, "Multilevel inverters: a survey of topologies, controls, and applications," *IEEE Transactions on Industrial Electronics*, vol. 49, no. 4, pp. 724–738, Aug 2002.

[6] D. G. Holmes and T. A. Lipo. Wiley-IEEE Press, 2003, pp. 1–744. [Online]. Available: http://ieeexplore.ieee.org/xpl/articleDetails.jsp?arnumber=5311953

[7] B. Wu and M. Narimani, *Cascaded H-Bridge Multilevel Inverters*. Wiley-IEEE Press, 2017, pp. 1–480. [Online]. Available: http://ieeexplore.ieee.org/xpl/articleDetails.jsp?arnumber=7827420

[8] M. Held, P. Jacob, G. Nicoletti, P. Scacco, and M. H. Poech, "Fast power cycling test of igbt modules in traction application," in *Proceedings of Second International Conference on Power Electronics and Drive Systems*, vol. 1, May 1997, pp. 425–430 vol.1.

[9] H. Huang and P. A. Mawby, "A lifetime estimation technique for voltage source inverters," *IEEE Transactions on Power Electronics*, vol. 28, no. 8, pp. 4113–4119, Aug 2013.

[10] M. Andresen, K. Ma, G. Buticchi, J. Falck, F. Blaabjerg, and M. Liserre, "Junction temperature control for more reliable power electronics," *IEEE Transactions on Power Electronics*, vol. 33, no. 1, pp. 765–776, Jan 2018.

[11] H. Lu, T. Tilford, C. Bailey, and D. R. Newcombe, "Lifetime prediction for power electronics module substrate mount-down solder interconnect," in *2007 International Symposium on High Density packaging and Microsystem Integration*, June 2007, pp. 1–10.

[12] I. F. Kovacevic, U. Drofenik, and J. W. Kolar, "New physical model for lifetime estimation of power modules," in *The 2010 International Power Electronics Conference - ECCE ASIA -*, June 2010, pp. 2106–2114.

[13] H. Salimian and H. Iman-Eini, "Fault-tolerant operation of three-phase cascaded h-bridge converters using an auxiliary module," *IEEE Transactions on Industrial Electronics*, vol. 64, no. 2, pp. 1018–1027, Feb 2017.

[14] M. Liserre, M. Andresen, L. Costa, and G. Buticchi, "Power routing in modular smart transformers: Active thermal control through uneven loading of cells," *IEEE Industrial Electronics Magazine*, vol. 10, no. 3, pp. 43–53, Sept 2016.

[15] Wintrich, U. Nicolai, W. Tursky, and T. Reimann, "Semikron application manual power semiconductors," 2011.

[16] Y. Ko, M. Andresen, G. Buticchi, and M. Liserre, "Power routing for cascaded h-bridge converters," *IEEE Transactions on Power Electronics*, vol. 32, no. 12, pp. 9435–9446, Dec 2017.

[17] ——, "Thermally compensated discontinuous modulation strategy for cascaded h-bridge converters," *IEEE Transactions on Power Electronics*, vol. 33, no. 3, pp. 2704–2713, March 2018.

[18] R. Burgos, G. Chen, F. Wang, D. Boroyevich, W. G. Odendaal, and J. D. V. Wyk, "Reliability-oriented design of three-phase power converters for aircraft applications," *IEEE Transactions on Aerospace and Electronic Systems*, vol. 48, no. 2, pp. 1249–1263, April 2012.

[19] M. Andresen, V. Raveendran, G. Buticchi, and M. Liserre, "Lifetime-based power routing in parallel converters for smart transformer application," *IEEE Transactions on Industrial Electronics*, vol. 65, no. 2, pp. 1675–1684, Feb 2018.

This article has been accepted for publication in a future issue of this journal, but has not been fully edited. Content may change prior to final publication. Citation information: DOI 10.1109/TIE.2018.2868304, IEEE Transactions on Industrial Electronics

$$v_{ab,c}(t) = \frac{2V_c^{dc}}{\pi}\Big[M_c\Big(-\phi+\pi-Z(1)\Big)+2Z(1/2)\Big]\cos(\omega_0 t)+\frac{2V_c^{dc}}{\pi}\sum_{n=2}^{\infty}\Big[2Z(a/2)-M_c\Big(Z(n)+Z(b)\Big)\Big]\cos(a\omega_0 t)$$
$$+\frac{8V_c^{dc}}{\pi^2}\sum_{m=1}^{\infty}\sum_{n=-\infty}^{\infty}\Bigg[J_a(m\pi M_c)\cos(c\pi)\Big(\pi-\phi-Z(a)\Big)$$
$$-\sum_{\substack{k=1\\ k\neq n,(if\,n>0)\\ k\neq 1-n,if(n\leq 0)}}^{\infty} J_{2k-1}(m\pi M_c)\cos\Big((m+k-1)\pi\Big)\Big(Z(d)+Z(e)\Big)\Bigg]\frac{cos(2m\omega_c t+a\omega_0 t)}{2m} \tag{8}$$

$$v_{ab,i}(t) = \frac{2V_i^{dc}}{\pi}\Big[M_c\Big(\frac{\phi+Z(1)}{2}\Big)+M_i\pi-Z(1/2)\Big]\cos(\omega_0 t)+\frac{2V_i^{dc}}{\pi}\sum_{n=2}^{\infty}\Big[-Z(a/2)+\frac{M_c}{2}\Big(Z(n)+Z(b)\Big)\Big]\cos(a\omega_0 t)$$
$$+\frac{8V_i^{dc}}{\pi^2}\sum_{m=1}^{\infty}\sum_{n=-\infty}^{\infty}\Bigg[\frac{1}{2}Z(a/2)J_0\Big(m\pi\Big(M_i+\frac{M_c}{2}\Big)\Big)\Big[cos(a\pi)sin\Big(\frac{3m\pi}{2}\Big)+sin\Big(\frac{m\pi}{2}\Big)\Big]$$
$$+\sum_{\substack{k=1\\ k\neq|2n-1|}}^{\infty} J_k\Big[m\pi\Big(M_i+\frac{M_c}{2}\Big)\Big[cos((a+k)\pi)sin\Big((3m+k)\frac{\pi}{2}\Big)+sin\Big((m+k)\frac{\pi}{2}\Big)\Big]\Big[\frac{1}{2}Z\Big(\frac{a+k}{2}\Big)+\frac{1}{2}Z\Big(\frac{a-k}{2}\Big)\Big]$$
$$+J_{|a|}\Big[m\pi\Big(M_i+\frac{M_c}{2}\Big)\Big[sin\Big((3m+|a|)\frac{\pi}{2}\Big)+sin\Big((m+|a|)\frac{\pi}{2}\Big)\Big]\Big[\frac{Z(a)}{2}+\frac{\phi}{2}\Big]$$
$$-\sum_{\substack{k=1\\ k\neq|2n-1|}}^{\infty} J_k\Big(m\pi M_i\Big)sin\Big((2m+k)\frac{\pi}{2}\Big)\Big(1+cos((a+k)\pi)\Big)\Big[\frac{1}{2}Z\Big(\frac{a+k}{2}\Big)+\frac{1}{2}Z\Big(\frac{a-k}{2}\Big)\Big]$$
$$-J_{|a|}\Big(m\pi M_i\Big)sin\Big((2m+|a|)\frac{\pi}{2}\Big)\Big(Z(a)-\pi+\phi\Big)\Bigg]\frac{cos(2m\omega_c t+a\omega_0 t)}{2m} \tag{9}$$

[20] Y. Shen, A. Chub, H. Wang, D. Vinnikov, E. Liivik, and F. Blaabjerg, "Wear-out failure analysis of an impedance-source pv microinverter based on system-level electro-thermal modeling," *IEEE Transactions on Industrial Electronics*, pp. 1–1, 2018.

[21] S. Kouro, P. Lezana, M. Angulo, and J. Rodriguez, "Multicarrier pwm with dc-link ripple feedforward compensation for multilevel inverters," *IEEE Transactions on Power Electronics*, vol. 23, no. 1, pp. 52–59, Jan 2008.

[22] Y. Cho, T. LaBella, J. S. Lai, and M. K. Senesky, "A carrier-based neutral voltage modulation strategy for multilevel cascaded inverters under unbalanced dc sources," *IEEE Transactions on Industrial Electronics*, vol. 61, no. 2, pp. 625–636, Feb 2014.

[23] J. Pou, D. Boroyevich, and R. Pindado, "New feedforward space-vector pwm method to obtain balanced ac output voltages in a three-level neutral-point-clamped converter," *IEEE Transactions on Industrial Electronics*, vol. 49, no. 5, pp. 1026–1034, Oct 2002.

[24] J. I. Leon, S. Vazquez, A. J. Watson, L. G. Franquelo, P. W. Wheeler, and J. M. Carrasco, "Feed-forward space vector modulation for single-phase multilevel cascaded converters with any dc voltage ratio," *IEEE Transactions on Industrial Electronics*, vol. 56, no. 2, pp. 315–325, Feb 2009.

[25] J. I. Leon, S. Vazquez, R. Portillo, L. G. Franquelo, J. M. Carrasco, P. W. Wheeler, and A. J. Watson, "Three-dimensional feedforward space vector modulation applied to multilevel diode-clamped converters," *IEEE Transactions on Industrial Electronics*, vol. 56, no. 1, pp. 101–109, Jan 2009.

[26] S. Lu, S. Mariéthoz, and K. A. Corzine, "Asymmetrical cascade multilevel converters with noninteger or dynamically changing dc voltage ratios: Concepts and modulation techniques," *IEEE Transactions on Industrial Electronics*, vol. 57, no. 7, pp. 2411–2418, July 2010.

[27] V. Naumanen, J. Luukko, P. Silventoinen, J. Pyrhönen, H. Sarén, and K. Rauma, "Compensation of dc link voltage variation of a multilevel series-connected h-bridge inverter," *IET Power Electronics*, vol. 3, no. 5, pp. 793–803, September 2010.

[28] M. Liserre, V. G. Monopoli, A. Dell'Aquila, A. Pigazo, and V. Moreno, "Multilevel phase-shifting carrier pwm technique in case of non-equal dc-link voltages," in *IECON 2006 - 32nd Annual Conference on IEEE Industrial Electronics*, Nov 2006, pp. 1639–1642.

[29] S. Li, Z. Yang, Q. Li, J. Gong, J. Sun, and X. Zha, "Asymmetrical phase-shifting carrier pulse-width modulation for harmonics suppression in cascaded multilevel converter under unbalanced dc-link voltages," in *2015 IEEE Energy Conversion Congress and Exposition (ECCE)*, Sept 2015, pp. 6804–6810.

[30] Y. Sun, J. Zhao, and Z. Ji, "An improved cps-pwm method for cascaded multilevel statcom under unequal losses," in *IECON 2013 - 39th Annual Conference of the IEEE Industrial Electronics Society*, Nov 2013, pp. 418–423.

[31] A. Marquez, J. I. Leon, S. Vazquez, R. Portillo, L. G. Franquelo, E. Freire, and S. Kouro, "Variable-angle phase-shifted pwm for multilevel three-cell cascaded h-bridge converters," *IEEE Transactions on Industrial Electronics*, vol. 64, no. 5, pp. 3619–3628, May 2017.

Vito Giuseppe Monopoli (S'98-M'05-SM'18) received the M.S. and PhD degrees in electrical engineering from the Bari Polytechnic, in 2000 and 2004, respectively. He is currently an Assistant Professor Bari Polytechnic, Bari, Italy.

His research activity concerns multilevel converters and the analysis of harmonic distortion produced by power converters and electrical drives. He is particularly interested in innovative control techniques for power converters. He is member of the IEEE Industry Applications Society, IEEE Industrial Electronics Society and IEEE Power Electronics Society.

$$
\begin{aligned}
v_o(t) &= v_{ab,c} + \sum_{i=1}^{2} v_{ab,i} = \\
&= \left[\frac{V_c^{dc}}{\pi}\Big[M_c\big[-\phi+\pi-Z(1)\big]+2Z(1/2)\Big] + \sum_{i=1}^{2}\left[\frac{V_i^{dc}}{\pi}\left[M_c\left(\frac{\phi+Z(1)}{2}\right)+M_i\pi-Z(1/2)\right]\right]\right]\cos(\omega_0 t) \\
&+ \left[\frac{V_c^{dc}}{\pi}\sum_{n=2}^{\infty}\left[2Z(a/2)-M_c\Big(Z(n)+Z(b)\Big)\right] + \sum_{i=1}^{2}\left[\frac{V_i^{dc}}{\pi}\sum_{n=2}^{\infty}\left[-Z(a/2)+\frac{M_c}{2}\Big(Z(n)+Z(b)\Big)\right]\right]\right]\cos(a\omega_0 t) \\
&+ \frac{4V_c^{dc}}{\pi^2}\sum_{m=1}^{\infty}\sum_{n=-\infty}^{\infty}\left[J_a(m\pi M_c)\cos(c\pi)\Big(\pi-\phi-Z(a)\Big)\right. \\
&\left. - \sum_{\substack{k=1 \\ k\neq n,(if\, n>0) \\ k\neq 1-n,(if\, n\leq 0)}}^{\infty} J_{2k-1}(m\pi M_c)\cos\Big((m+k-1)\pi\Big)\Big(Z(d)+Z(e)\Big)\right]\frac{\cos(2m\omega_c t+a\omega_0 t)}{2m} \\
&+ \sum_{i=1}^{2}\left[\frac{4V_i^{dc}}{\pi^2}\sum_{m=1}^{\infty}\sum_{n=-\infty}^{\infty}\left[\frac{1}{2}Z(a/2)J_0\Big(m\pi\Big(M_i+\frac{M_c}{2}\Big)\Big)\Big[cos(a\pi)sin\Big(\frac{3m\pi}{2}\Big)+sin\Big(\frac{m\pi}{2}\Big)\Big]\right.\right. \\
&+ \sum_{\substack{k=1 \\ k\neq|2n-1|}}^{\infty} J_k\left[m\pi\Big(M_i+\frac{M_c}{2}\Big)\left[cos((a+k)\pi)sin\Big((3m+k)\frac{\pi}{2}\Big)+sin\Big((m+k)\frac{\pi}{2}\Big)\right]\left[\frac{1}{2}Z\Big(\frac{a+k}{2}\Big)+\frac{1}{2}Z\Big(\frac{a-k}{2}\Big)\right]\right. \\
&+ J_{|a|}\left[m\pi\Big(M_i+\frac{M_c}{2}\Big)\Big[sin\Big((3m+|a|)\frac{\pi}{2}\Big)+sin\Big((m+|a|)\frac{\pi}{2}\Big)\Big]\Big[\frac{Z(a)}{2}+\frac{\phi}{2}\Big]\right. \\
&- \sum_{\substack{k=1 \\ k\neq|2n-1|}}^{\infty} J_k\Big(m\pi M_i\Big)sin\Big((2m+k)\frac{\pi}{2}\Big)\Big(1+cos((a+k)\pi)\Big)\left[\frac{1}{2}Z\Big(\frac{a+k}{2}\Big)+\frac{1}{2}Z\Big(\frac{a-k}{2}\Big)\right] \\
&\left.\left.\left. - J_{|a|}\Big(m\pi M_i\Big)sin\Big((2m+|a|)\frac{\pi}{2}\Big)\Big(Z(a)-\pi+\phi\Big)\right]\frac{\cos(2m\omega_c t+a\omega_0 t)+2m\theta_i}{2m}\right. \qquad (10)
\end{aligned}
$$

Abraham Marquez (S'14-M'16) was born in Huelva, Spain, in 1985. He received his B.S. and M.S. degrees in telecommunications engineering in 2014 and 2016 from the Universidad de Sevilla (US), Spain, where he is currently working toward the PhD degree in electronic engineering.

His main research interest are modulation techniques, multilevel converters, power conversion for renewable energy sources and model-based predictive control of power converters and drives. Mr. Marquez was recipient as coauthor of the 2015 Best Paper Award of the IEEE Industrial Electronics Magazine.

Jose I. Leon (S'04-M'07-SM'14-F'17) was born in Cadiz, Spain. He received the B.S., M.S., and PhD degrees in telecommunications engineering from Universidad de Sevilla (US), Seville, Spain, in 1999, 2001, and 2006, respectively. Currently, he is an Associate Professor with the Department of Electronic Engineering, US.

His research interests include modulation and control of power converters for high-power applications and renewable energy systems. He is currently serving as an Associate Editor of the IEEE Transactions on Industrial Electronics. Dr. Leon was a co-recipient of the 2008 Best Paper Award of IEEE Industrial Electronics Magazine, the 2012 Best Paper Award of the IEEE Transactions on Industrial Electronics, and the 2015 Best Paper Award of IEEE Industrial Electronics Magazine. He was the recipient of the 2014 IEEE J. David Irwin Industrial Electronics Society Early Career Award, the 2017 IEEE Bimal K. Bose Energy Systems Award and the 2017 Manuel Losada Villasante Award for excellence in research and innovation. In 2017 he has been elevated to the IEEE fellow grade with the following citation "for contributions to high-power electronic converters".

Youngjong Ko (S'16) received his B.S. and M.S. degrees in Electronic Engineering from the Ajou University, Suwon, Korea in 2009 and 2012, respectively. Since 2015 he is working toward his Ph.D degree from the chair of power electronics at the Kiel University, Germany.

His research interests include grid-connected power converter and reliability in power electronics.

Giampaolo Buticchi (S'10-M'13-SM'17) received the Master degree in Electronic Engineering in 2009 and the PhD degree in Information Technologies in 2013 from the University of Parma, Italy. In 2012 he was visiting researcher at The University of Nottingham, UK. Between 2014 and 2017 he was a post-doctoral researcher at the University of Kiel, Germany. He is now Associate Professor in Electrical Engineering at The University of Nottingham Ningbo China.

His research focuses on power electronics for renewable energy systems, smart transformer fed micro-grids and dc grids for the More Electric Aircraft. He is author/co-author of more than 160 scientific papers.

Marco Liserre (S'00-M'02-SM'07-F'13) received the M.S. and PhD degree in Electrical Engineering from the Bari Polytechnic, respectively in 1998 and 2002. He has been Associate Professor at Bari Polytechnic and from 2012 Professor in reliable power electronics at Aalborg University (Denmark). From 2013 he is Full Professor and he holds the Chair of Power Electronics at Kiel University (Germany), where he leads a team of more than 20 researchers with an annual budget of 2 Mill. Euro and cooperation with 20 companies. He has published over 350 technical papers (more than 110 of them in international peer-reviewed journals) and a book. These works have received more than 25000 citations. Marco Liserre is listed in ISI Thomson report "The world's most influential scientific minds" from 2014.

He has been awarded with an ERC Consolidator Grant for the project "The Highly Efficient And Reliable smart Transformer (HEART), a new Heart for the Electric Distribution System" and with the ERC Proof of Concept Grant U-HEART.

He is member of IAS, PELS, PES and IES. He has been serving all these societies in different capacities. He has received the IES 2009 Early Career Award, the IES 2011 Anthony J. Hornfeck Service Award, the 2014 Dr. Bimal Bose Energy Systems Award, the 2011 Industrial Electronics Magazine best paper award the Third Prize paper award by the Industrial Power Converter Committee at ECCE 2012, 2012, the 2017 IEEE PELS Sustainable Energy Systems Technical Achievement Award and the 2018 IEEE IES Mittelmann Achievement Award which is the highest award of the IEEE-IES.